Acid or salt adaptation of Listeria monocytogenes 10403S grown until exponential phase aerobically, enhances sensitivity to oxidative stress

Journal of Applied Microbiology, 2025, 136(7), lxaf173
https://doi.org/10.1093/jambio/lxaf173
Advance access publication date: 14 July 2025
Research Article

JOURNAL OF APPLIED MICROBIOLOGY
OXFORD UNIVERSITY PRESS

Acid or salt adaptation of *Listeria monocytogenes* 10403S grown until exponential phase aerobically, enhances sensitivity to oxidative stress

Marcia Boura[1,‡], Mahide M. Yilmaz Topcam[1,‡], David Spiteri[2,3], Carolina Bruschi[1], Vasileios Valdramidis[2,3], Kimon A.G. Karatzas[1,*]

[1]Department of Food and Nutritional Sciences, University of Reading, Reading, RG6 6AD, United Kingdom
[2]Department of Food Sciences and Nutrition, Faculty of Health Sciences, University of Malta, Msida, MSD 2080, Malta
[3]Centre of Molecular Medicine and Biobanking, University of Malta, Msida, MSD 2080, Malta

*Corresponding author: Department of Food and Nutritional Sciences, University of Reading, Whiteknights, PO Box 226 Reading, RG6 6AD, United Kingdom. E-mail: k.karatzas@reading.ac.uk
‡These authors contributed equally to this work.

Abstract

Aims: The work aimed at investigating a possible role of *sigB* in catalase transcription and activity in *Listeria monocytogenes*. Furthermore, we also aimed to investigate whether *sigB* upregulation during the exponential phase, due to acid or salt adaptation, could result in hypersensitivity to oxidative stress. Finally, we investigated how this discovery could be used in the wider concept of Hurdle Technology through combination of different stresses.

Methods and results: *Listeria monocytogenes* 10403S WT and Δ*sigB* strains were grown aerobically, and catalase transcription and activity were assessed at different growth stages. Catalase transcription peaked at 6 h of growth in both strains, with Δ*sigB* showing higher levels. Subsequently, from 8 to 10 h, a major drop to similarly low levels occurred for both strains. However, catalase activity peaked 2 h later (at 8 h of growth) than transcription and remained higher in Δ*sigB* beyond this point. To evaluate stress adaptation, exponential-phase cells were exposed to sub-lethal acidic conditions (pH 4.5; HCl) or salt (0.5 mol l^{-1} NaCl) and later subjected to H_2O_2 or sonication (tested only with acid). Adaptation increased sensitivity in the wild type (WT) but not in Δ*sigB,* underpinning the negative role of *sigB* upregulation. Acid adaptation reduced catalase activity in both strains, explaining the reduced oxidative stress resistance, although salt adaptation did not affect catalase activity. After adaptation to acid or salt, application of oxidative stress without removing the initial adaptation stresses resulted in a higher synergistic effect in both WT and Δ*sigB*.

Conclusion: The above synergistic effects are important for our understanding of listerial oxidative stress resistance and optimization of relevant oxidative stress decontamination processes (e.g. oxidative compounds, ultrasound, and plasma treatments) but also virulence.

Impact Statement

The results obtained in this study, are important for the food industry, especially for the optimization of oxidative stress-based processes but also for the understanding of listerial stress adaptation, resistance, and virulence.

Keywords: food safety; transcriptional regulation; sigma B; acid stress; hurdle technology; ultrasound; NaCl; stress adaptation; acid adaptation; salt adaptation

Introduction

Listeria monocytogenes is a Gram-positive bacteria that is ubiquitous in nature and found in fresh or processed foods, causing listeriosis a life-threatening food-borne illness, (Ramaswamy et al. 2007, McLaughlin et al. 2011, Quereda et al. 2021). In the natural environment, *L. monocytogenes* is often exposed to a wide range of environmental stresses, such as acidic conditions, high salt concentrations, increased temperatures, or oxidative stress. These stresses are also often employed during disinfection and processing in food preparation premises or food treatment [e.g. plasma, ultrasound (Ferreira et al. 2001, Moorhead and Dykes 2003, Sue et al. 2004)]. Through evolution, *L. monocytogenes* has developed a stress defence machinery to cope with adverse environmental conditions. This machinery normally protects *L. monocytogenes* against multiple stresses following exposure to one, at a level where no sublethal injury occurs. For example, exposure to sublethal acid conditions induces cross-resistance to multiple other stresses (Lou and Yousef 1997, Davidson and Harrison 2002, Bonnet and Montville 2005, Skandamis et al. 2012, Shen et al. 2015).

In Gram-positive bacteria such as *L. monocytogenes*, survival in a wide range of hostile environments is widely attributed to the alternative sigma factor SigB, a well-studied transcriptional regulator, responsible for regulating the expression of >150 stress genes (Abram et al. 2008). SigB-dependent genes are being upregulated upon entrance in the stationary phase of growth, as well as in response to a variety of environmental conditions, including acid stress (Ferreira et al. 2001, Sue et al. 2004, Wemekamp-Kamphuis et al. 2004, Chaturongakul and Boor 2006, Ondrusch and Kreft 2011, Cortes et al. 2020), osmotic stress (Ferreira et al. 2001,

Received 21 January 2025; **revised** 23 May 2025; **accepted** 12 July 2025

Kazmierczak et al. 2003, Abram et al. 2008, Utratna et al. 2012, 2014), heat shock, photo-oxidative, and oxidative stress (Chaturongakul and Boor 2006, Oliver et al. 2010, Ondrusch and Kreft 2011, Utratna et al. 2014, Boura et al. 2016). It has also been shown that *L. monocytogenes* mutants lacking *sigB* are sensitive to a variety of stresses, such as acidic conditions, bile salts, and osmotic conditions (Ferreira et al. 2001, 2004, Oliver et al. 2010).

However, the role of *sigB* in oxidative stress during stationary phase has been controversial (Boura et al. 2016), as several studies reported a protective role for *sigB* (Heisick et al. 1989, Ferreira et al. 2001, Oliver et al. 2010), while others find no significant role (Oliver et al. 2013). These differences were mainly attributed to strain-specific effects (Oliver et al. 2013). However, subsequently, we explained that these discrepancies were at least partly due to low oxygen levels in the cultures used in these experiments. When we grew cells aerobically, we were able to show in two different *L. monocytogenes* strains, EGD-e and 10403S, that under aerobic conditions, the presence of *sigB* results in increased sensitivity to hydrogen peroxide (Boura et al. 2016). Furthermore, we found that the presence of *sigB* negatively affected catalase activity in stationary phase, explaining the above effect. We also observed that the effect of SigB on oxidative stress depended on the stage of growth and the oxygen levels during growth.

Knowledge of the behaviour of *L. monocytogenes* under multiple stresses is highly valuable for Hurdle Technology as the latter involves the application of multiple stresses, either simultaneously or sequentially. This knowledge could contribute to a deeper understanding of the role and impact of environmental conditions and stresses on the behaviour of this pathogen against oxidative stress. It could also help in optimization of existing food processes or in invention of new processes (new stress combinations) to eliminate microbes in food. Furthermore, oxidative stress occurs during phagocytosis and as such, it is also important for a better understanding of listerial virulence. For example, the hypersensitivity observed in the presence of *sigB* could explain the possible lack of a role for *sigB* in intracellular proliferation (Chatterjee et al. 2006, Boura et al. 2016) and the lack of a major intracellular upregulation, as this would render cells sensitive to oxidative stress in the phagocytic vacuole (Chatterjee et al. 2006, Schultze et al. 2015).

Therefore, in the present work, to explain the above phenomena, we examined catalase transcription and activity at different time points during growth. This analysis aimed to explain the hypersensitivity observed in the presence of *sigB* during stationary phase. Furthermore, we looked if *sigB* upregulation during exponential phase could result in a similar effect, by adapting cells to sublethal levels of acid and salt before exposure to lethal oxidative stress. Both approaches reflect the conditions in the environment or food, where cells encounter multiple stresses. Since catalase was shown to be an important parameter in the role of *sigB* in oxidative stress, we also measured catalase activity.

Materials and methods

Bacterial strains and culture conditions

All experiments were performed with *L. monocytogenes* 10403S (Karatzas et al. 2010) and its corresponding isogenic Δ*sigB* mutant (Wiedmann et al. 1998). All strains were stored at −80°C in an aqueous solution of 15% (v/v) dimethyl sulfoxide from where stock cultures were prepared by streaking onto Brain Heart Infusion (BHI) agar (1% m/v; Lab M—NEOGEN, Lancashire, UK) and incubated at 37°C overnight. Three colonies were picked from each strain's stock culture and all three were inoculated in one universal containing 3 ml BHI broth (Lab M—NEOGEN, Lancashire, UK), to prepare the pre-experimental first overnight culture. In all cases, experiments were performed at least in triplicate, and as such, at least three of the above cultures were prepared for each experiment. These cultures were grown until the stationary phase of growth at 37°C and 120 rpm, and each one was inoculated at 1% in the same medium and under the same growth conditions (37°C at 120 rpm), to prepare each experimental culture. Experimental cultures were in 20 ml medium, grown in conical flasks (250 ml) until the specific time needed depending on the experiment.

Catalase activity assays

For temporal catalase activity analysis, *L. monocytogenes* cultures were grown as described above for 4, 6, 8, 14, and 18 h. Catalase activity was assessed as described previously (Iwase et al. 2013), with minor modifications. One millilitre of bacterial culture was centrifuged for 3 min at 10 000 × *g*, and the supernatant was carefully removed without disturbing the pellet. In the temporal analysis, it was important to make comparisons between different stages of growth, where cell concentrations were different. Therefore, centrifugation with biomass normalization was employed to adjust for the number of cells, which would allow for comparisons between different stages of growth.

The pellet was resuspended in phosphate buffer (pH7; 100 μl per 10 mg of pellet), and 100 μl was transferred to a test tube containing 100 μl of 1% (v/v) Triton X-100 (Sigma–Aldrich, Dorset, UK). A volume of 100 μl of H_2O_2 (30% v/v) was then added to each test tube. Oxygen released during the enzymatic degradation of H_2O_2 was measured as the column of foam formed. The addition of Triton X-100 stabilized the bubbles formed, allowing an accurate measurement of the oxygen released. After 5 min, the column height of the foam was measured and, in parallel, photographic images were taken to estimate the foam's height, which was proportional to the oxygen levels produced by the catalase reaction. All samples were also analysed omitting the centrifugation step.

Additional catalase activity assays were performed in parallel with the survival experiments to identify the possible role of catalase in the oxidative stress resistance, following stress adaptation. In this case, no cell number or weight adjustment was performed as we already had ensured that cultures had the same number of cells, and no adjustment was required. For every culture used in the survival experiments, a duplicate culture was prepared with the same inoculum, grown in parallel, and exposed to acid or salt adaptation as described below. Subsequently, one of the cultures was used to assess survival under oxidative stress, and its duplicate was used to assess catalase activity. A volume of 100 μl of 1% (v/v) Triton X-100 (Sigma–Aldrich, Dorset, UK) was added to 100 μl of these cultures and subsequently, 100 μl H_2O_2 (30% v/v) were then added to each test tube. Subsequently, the height of the foam was recorded. All these experiments were performed in triplicate.

Table 1. Primers used in this study.

Name[a]	Sequence (5′ → 3′)	Efficiency
katF	CGCACGGGAAATTTGTTACT	2.05
katR	GGTCAGGCTTCAAGGAATGA	
16SF	TGGGGAGCAAACAGGATTAG	2.27
16SR	TAAGGTTCTTCGCGTTGCTT	

[a]Primers designed based on the *L. monocytogenes* 10403S and were adopted from Boura et al. (2016).

Catalase gene expression

Temporal catalase (*kat*) transcription during the different stages of growth was assessed for the 10403S WT and its corresponding isogenic Δ*sigB* mutant, as described previously (Karatzas et al. 2010) using real-time reverse transcription quantitative polymerase chain reaction (RT-qPCR). The primers used (Table 1) were identical to those used previously, (Boura et al. 2016), while the primer efficiency (Table 1) was close to 2, and these values were used for efficiency correction in the quantification step. Bacterial cultures, of both WT and Δ*sigB*, were grown aerobically in conical flasks (120 rpm at 37°C). Samples for RNA isolation were collected along the growth curve at 4, 6, 8, and 10 h of growth and immediately mixed with chilled phenol/ethanol (5/95%) solution. We did not analyse any time points beyond 10 h, as catalase activity did not show any major difference beyond 8–10 h of growth (Fig. 1).

The samples in the phenol/ethanol mix were centrifuged at 4°C, 5000 ×*g* for 10 min and the pellet was stored at −80°C until usage. Subsequently, the pellet was processed as described in the RNeasy Midi kit (Qiagen, Manchester, UK). DNA contamination was removed with the Turbo DNA-free Kit (Ambion, Life Technologies, ThermoFisher Scientific, Paisley, UK), and the RNA concentration was quantified using a NanoDrop spectrophotometer (Thermo Fisher Scientific, Paisley, UK). The RNA concentration was normalized (0.5 μg of RNA) and converted to cDNA using random primers, and the SuperScript II Reverse Transcriptase Kit (Invitrogen, ThermoFisher Scientific, Paisley, UK). The cDNA was then stored at −20 °C until further use.

Relative expression was calculated as the ratio between the expression of the target gene (*kat*) and the expression of the 16S rRNA gene, which served as the reference gene in each cDNA sample. Calculations were carried out using the advanced relative quantification analysis settings of the LightCycler 480 software program, with PCR efficiency correction performed as described previously (Karatzas et al. 2010). The relative expression of each gene was calculated by a comparison of its expression relative to that of the 16S rRNA gene. For the presentation of the results, we identified the highest of all the values, set that value arbitrarily as 100%, and then all other ones were adjusted accordingly relative to this maximum value.

Survival following adaptation to acid stress and cell transfer to lethal H_2O_2 or ultrasound challenge

All survival experiments were performed with cells at the exponential phase of growth (5 h). The exponential phase for WT was defined at ∼5 h of growth, determined using the Baranyi and Roberts model (data not shown; Baranyi et al. 1996, Baranyi and Roberts 1994). *Listeria monocytogenes* 10403S cultures were grown in BHI broth at 37°C with shaking (120 rpm) until the exponential phase (5 h of growth and ∼7–8 log CFU ml^{-1}). Subsequently, cultures were adapted to mild acidic conditions (HCl, pH 4.5) for 30 min while non-acid-adapted controls were left untouched for these 30 min

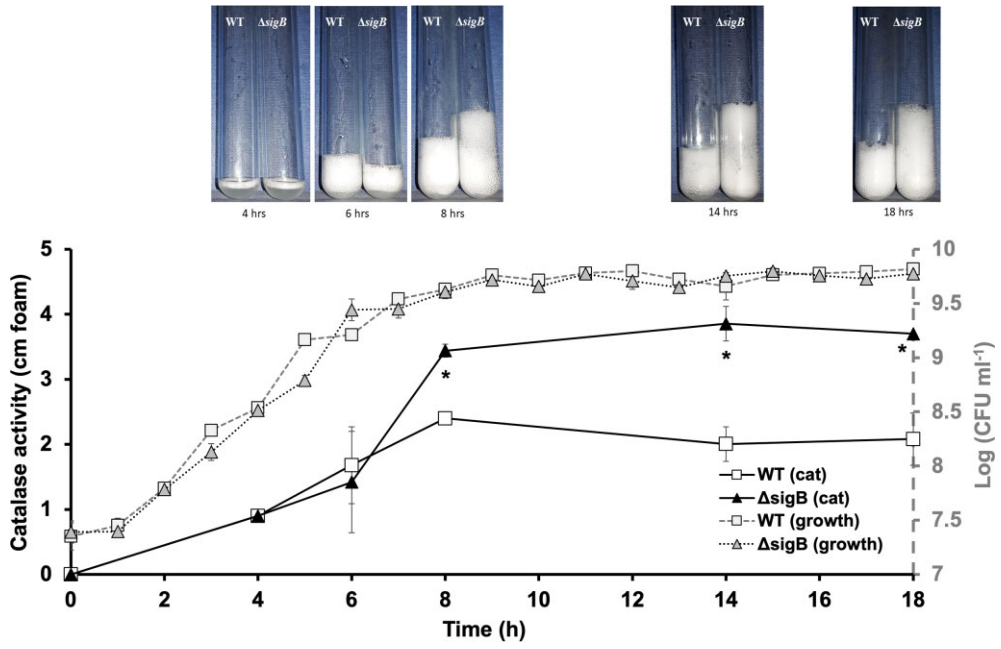

Figure 1. Catalase activity (portrayed on the primary *y*-axis with black line on the left side) of 10403S WT (□; continuous black line) and Δ*sigB* (▲; continuous black line) at different stages of growth (portrayed on the secondary *y*-axis with dashed grey line on the left side) for WT 10403S (■; dashed grey line) and Δ*sigB* (▲; dashed grey line) at 37°C aerobically (120 rpm). Tests were performed with the addition of 100 μl of 30% H_2O_2 to 10 mg of a bacterial pellet resuspended in a mix 1:1 PBS (1X) and triton X-100 (1X). Assays were performed in triplicate and asterisk (*) indicates a statistically significant difference between the WT and Δ*sigB* (*t*-test; $P < 0.05$). Photos portray one out of three biological replicates on which catalase activity tests were performed.

(5.5 h total incubation). Then, acid-adapted and control cultures were harvested by centrifugation (4723 × *g* for 10 min, 37°C). Cell pellets were resuspended in fresh BHI (pH 7.2) and either immediately challenged with 1.5% H_2O_2 for 60 min (use of 30% v/v H_2O_2) or subjected to ultrasound treatment. Samples were analysed through the preparation of decimal dilutions and plating onto BHI agar followed by incubation for 24 h at 37°C and enumeration.

For ultrasound treatment, the sample was pipetted into 100 ml of sterile distilled water and used for ultrasound treatment in biological triplicates. Ultrasound treatment was conducted in a Hielscher UP200St Ultrasonifier equipped with a generator UP200St-G 200 W and a transducer UP200St-T, operating at a constant frequency of 26 kHz and a 14-mm diameter sonotrode. For each sample, the working solution was transferred into a 500 ml jacketed beaker, attached to a water pump. The beaker was carefully disinfected with alcohol between each experiment. Then, the tip of the sonotrode was placed in the centre of the beaker, containing 100 ml of bacterial suspension, and submerged to a depth of 1 cm. All samples were treated for 5 min in the continuous mode at 100% intensity and Ultrasonic Intensity of 31.89 W/cm^2. Temperature was kept below 45°C, to eliminate the impact of the thermal process during ultrasound treatment on microbial survival, by circulating cold water continuously to lower delta T. Temperature records were obtained with the use of PT100 probe to ensure that during the experiments the temperature did not exceed the 45°C.

To standardize the intensity level of the ultrasound process due to different ultrasound devices, ultrasound intensity (UI; expressed as W/cm^2) for the ultrasonic horn was calculated. The UI can be determined calorimetrically using the following equations that were described by Mason (1999).

$$\mathrm{UI} = \frac{4P}{\pi d^2}, \tag{1}$$

where d [cm] is the diameter of the sonotrode.

In the above equation, P [W] represents the absolute ultrasonic power and can be defined as

$$P = mC_p\left(\frac{dT}{dt}\right)_{x=0}, \tag{2}$$

where, m [g] is the mass, C_p [J/g·K] is the specific heat capacity, and dT/dt [K/s] is the ratio of change of temperature during sonication. Where:

$m = 100$ g,
$Cp = 4.179$ J/g °C,
$dT/dt = 0.1179$ °C/s,
$d = 1.4$ cm.

Following ultrasound treatment, samples were collected, and decimal serial dilutions were prepared and plated onto BHI agar. Subsequently, plates were incubated overnight at 37°C and colony counts were assessed to identify the level of inactivation induced by the ultrasound treatment.

Survival following adaptation to acid or salt and cell transfer to lethal H_2O_2 challenge (*first approach*)

As mentioned above, all survival experiments were performed with exponential phase cells (5 h of growth; Baranyi and Roberts 1994, Baranyi et al. 1996). To assess the role of acid and salt adaptation on oxidative stress resistance, two approaches were followed. As one of our aims was to assess the role of SigB in these stresses, the levels of adaptation conditions selected were not lethal, but they were stressful enough to upregulate *sigB* and activate the SigB operon. The sublethal conditions were selected based on previous works (Ferreira et al. 2001, Kazmierczak et al. 2003, Sue et al. 2004, Wemekamp-Kamphuis et al. 2004, Chaturongakul and Boor 2006, Abram et al. 2008, Utratna et al. 2012, 2014).

The ***first approach*** was identical to that described with the ultrasound experiments, but with the inclusion of the Δ*sigB* mutant together with the WT, to assess the role of SigB in acid and salt adaptation and oxidative stress resistance. In brief, the cells were grown in BHI broth at 37°C with shaking (120 rpm) until the exponential phase (5 h of growth and ∼7–8 log CFU ml^{-1}). Subsequently, cultures were adapted to mild acidic conditions (HCl, pH 4.5) for 30 min or salt (0.5 mol l^{-1} NaCl) conditions for 60 min. At this point in the ***first approach***, stress-adapted cell cultures, together with their corresponding non-adapted controls were harvested by centrifugation (4723 × *g* for 10 min, 37 °C), and removed from the adaptation stress environment. Subsequently, cell pellets were resuspended in fresh BHI and immediately challenged with the use of different concentrations of 30% (v/v) H_2O_2. Based on the different oxidative stress resistance of the strains, for these survival experiments, final concentrations of 1.5% and 0.8% H_2O_2 for WT and Δ*sigB* were used for acid-adapted cells. For salt-adapted cells salt and their corresponding controls, the concentrations of 2.2% and 1.6% (v/v) were used for WT and Δ*sigB*. Cell viability was assessed by taking samples at regular time intervals during the H_2O_2 challenge by preparing and plating decimal dilutions in BHI agar. Agar plates were incubated at 37°C for 24 h and colony-forming units (CFUs) were enumerated to assess the concentration of bacteria at each time point. Results are presented as means of three biological replicates.

Survival following adaptation to acid or salt and exposure to lethal hydrogen peroxide stress with maintenance of the adaptation stress (*second approach*)

Furthermore, we assessed the effect of the lethal oxidative stress applied following the adaptation to either acidic or salt sublethal stress, but without cell transfer by omitting the subsequent harvesting centrifugation step after the adaptation period. This resulted in the lethal oxidative stress challenge coinciding with the adaptation stress after the adaptation was concluded.

Overall, in this ***second approach***, cells were adapted for 30 min (acid) and 60 min (salt) under the same pH and salt environments as the ones for the ***first approach*** in parallel with non-stress-adapted controls. Subsequently, acid-adapted WT and Δ*sigB* cells and their corresponding non-stress-adapted controls were challenged with 30% (v/v) H_2O_2 to a final concentration of 0.5% and 0.35% (v/v). Salt-adapted WT and Δ*sigB* and their corresponding controls were challenged with 1.5% and 1.25% (v/v). As in the ***first approach***, different H_2O_2 concentrations were used due to different oxidative stress resistance of cells. The presence of the adaptation stress coinciding with the lethal H_2O_2 challenge stress, made cells highly sensitive and therefore, overall lower H_2O_2 concentrations had to be used compared to the ***first approach***. As in the ***first approach***, in every survival assay and every H_2O_2

concentration used, non-adapted WT and Δ*sigB* were always included.

Cell viability was assessed by taking samples at regular time intervals and plating decimal serial dilutions onto BHI agar. Agar plates were incubated at 37°C for 24 h and CFUs were enumerated to assess the concentration of bacteria at each time point. Results are presented as means of three biological replicates, each performed in triplicate.

Statistical analysis

All experiments were performed at least in triplicate (three biological replicates and three technical replicates) unless stated otherwise, and differences between groups were assessed using paired *t*-test, with $P < 0.05$ being considered statistically significant.

Results

Catalase activity during growth

In previous work, we have shown that catalase activity depends on the phase of growth and the presence of *sigB* (Boura et al. 2016). Therefore, in the present study, we performed a temporal analysis of the catalase activity during the growth of WT and Δ*sigB*. Catalase activity measured with cell biomass adjustment, was low in both WT and Δ*sigB* during the lag and early exponential phase (4 h; Fig. 1). At the late exponential phase of growth (6 h), both strains showed some catalase activity, which was higher in the WT, although this was without statistical significance ($P > 0.05$). At the early stationary phase (8 h), WT had lower catalase activity than Δ*sigB* ($P < 0.05$) and remained as such thereafter (10, 14, and 18 h; Fig. 1). At the stationary phase (8–18 h), catalase activity appeared to be stable in both strains and significantly higher in Δ*sigB* ($P < 0.05$; Fig. 1).

Catalase (*kat*) transcription during *L. monocytogenes* growth

Along with the temporal analysis of catalase activity, we also performed a temporal analysis of catalase (*kat*) transcription but only until 10 h of growth since beyond this point, no major changes in catalase activity occurred (Fig. 1). A major expression peak occurred at 6 h of growth, which was significantly higher in Δ*sigB* ($P < 0.05$) than the WT. This peak was followed by a major drop at low and similar levels for both strains at 8 h of growth (early stationary phase; Fig. 2). A similar trend without any difference between the two strains was also observed at 10 h of growth (Fig. 2).

Survival following adaptation to acid stress and cell transfer to lethal H_2O_2 or ultrasound challenge

Following the temporal analysis of catalase activity and transcription, the effect of acid adaptation on the survival of WT was evaluated against lethal H_2O_2 oxidative stress and ultrasound, which also exerts antimicrobial effects mediated by oxidative stress (Spiteri et al. 2017). Acid-adapted cells (HCl; pH 4.5 for 30 min), harvested and resuspended in fresh BHI (pH 7.2) showed significantly lower resistance to H_2O_2 with a dramatic 5.98 log reduction compared to no reduction for non-adapted controls (Fig. 3a). Subsequently, we looked at the effect of ultrasound and acid-adapted cells also showed lower resistance to ultrasound, having a 3.4 log reduction of CFU

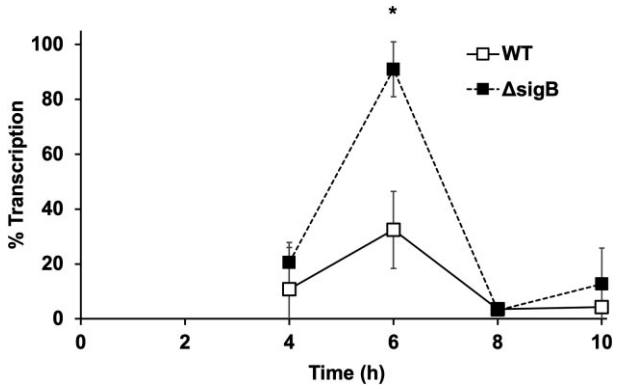

Figure 2. Expression of *kat* gene in 10403S WT (□; continuous black line) and Δ*sigB* (■, dashed black line), at different stages of growth under 37°C aerobically (120 rpm). The percentage of expression was calculated for each replicate by normalizing *kat* relative expression against the highest value, which was arbitrarily set as 100%. The asterisk denotes a statistically significant difference ($P \leq 0.05$) between WT and Δ*sigB*. Error bars represent mean standard deviations of three individual experiments.

ml^{-1} ($P < 0.05$) compared to 0.6 and −0.1 log reduction of CFU ml^{-1} for ultrasound and the acid adaptation treatment alone, respectively (Fig. 3b).

Survival following adaptation to acid and cell transfer to lethal H_2O_2 challenge (*first approach*)

Acid-adapted WT cells (HCl; pH 4.5 for 30 min) from the exponential phase of growth showed statistically significant lower resistance to 1.5% H_2O_2, having a 5.6 log reduction of CFU ml^{-1} ($P < 0.05$), 30 min after the challenge, while cell numbers of the non-acid adapted control were not affected ($P > 0.05$; Fig. 4a). Non-adapted Δ*sigB* control showed complete inactivation within 30 min (no counts recovered; Fig. 4a) and was more sensitive than the WT.

Acid-adapted Δ*sigB* from the exponential phase of growth did not show a statistically significant difference in survival to 0.8% H_2O_2, compared to the non-adapted control (Fig. 4b), as they showed a 3.4 and 2.19 log reduction, respectively. Non-adapted WT showed no reduction after 60 min (Fig. 4b), and as such, it was significantly more resistant than Δ*sigB*.

Survival following adaptation to acid and exposure to lethal H_2O_2 stress with maintenance of the adaptation stress (*second approach*)

We also performed experiments with a similar acid adaptation (HCl; pH 4.5 for 30 min) conditions as the ones described in the ***first approach*** but omitted the harvesting-centrifugation step and applied the lethal H_2O_2 challenge in the presence of the acidic conditions, resulting in the two stresses coinciding (***second approach***). Final concentrations of 0.5% and 0.35% H_2O_2 were used for both WT and Δ*sigB* (Fig. 5).

Acid-adapted WT was sensitive to 0.5% as it showed a 4.9 log reduction in 60 min, while no inactivation occurred in the WT without any adaptation (Fig. 5a). Non-adapted Δ*sigB* showed complete inactivation within 30 min (no counts recovered; Fig. 5a) and as such, was more sensitive than the WT.

Interestingly, at 0.35% H_2O_2, Δ*sigB* showed similar behaviour to WT, as adaptation to acid rendered it sensitive to the lethal H_2O_2 when the sublethal acidic conditions were

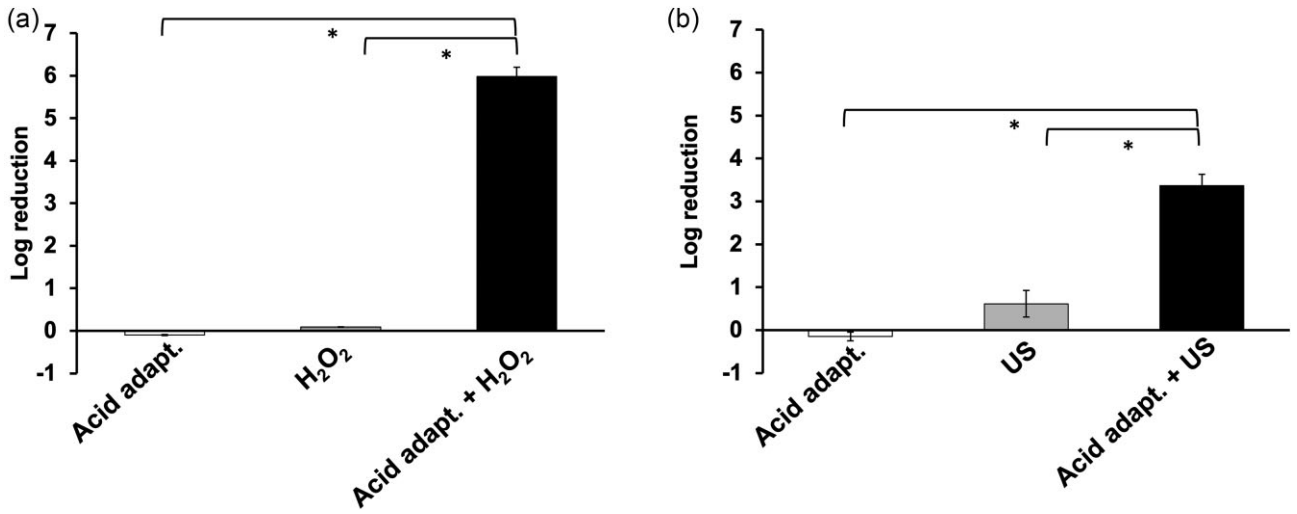

Figure 3. Effect of acid adaptation (HCl) on H_2O_2 resistance (a) and ultrasound resistance (b) of exponential phase cultures of *L. monocytogenes* 10403S WT with sequential application of the stresses (***first approach***). WT 10403S was grown in BHI broth until the exponential phase and were either adapted to sublethal acid stress (HCl) at pH 4.5 (acid adaptation) or left untouched as controls for 30 min. They were subsequently harvested, resuspended in fresh BHI (pH 7.2) and subjected to 1.5% H_2O_2 for 60 min (acid adaptation + H_2O_2; black bar; A), or a 3 min ultrasound treatment (Acid adapt. + US; black bar; B), while non-acid adapted controls were subjected to similar H_2O_2 (H_2O_2; grey bar; A) and ultrasound (US; grey bar, B) treatments. Asterisks represent statistically significant difference ($P \leq 0.01$). Error bars represent standard deviation of three independent biological replicates, while each comprised three technical replicates.

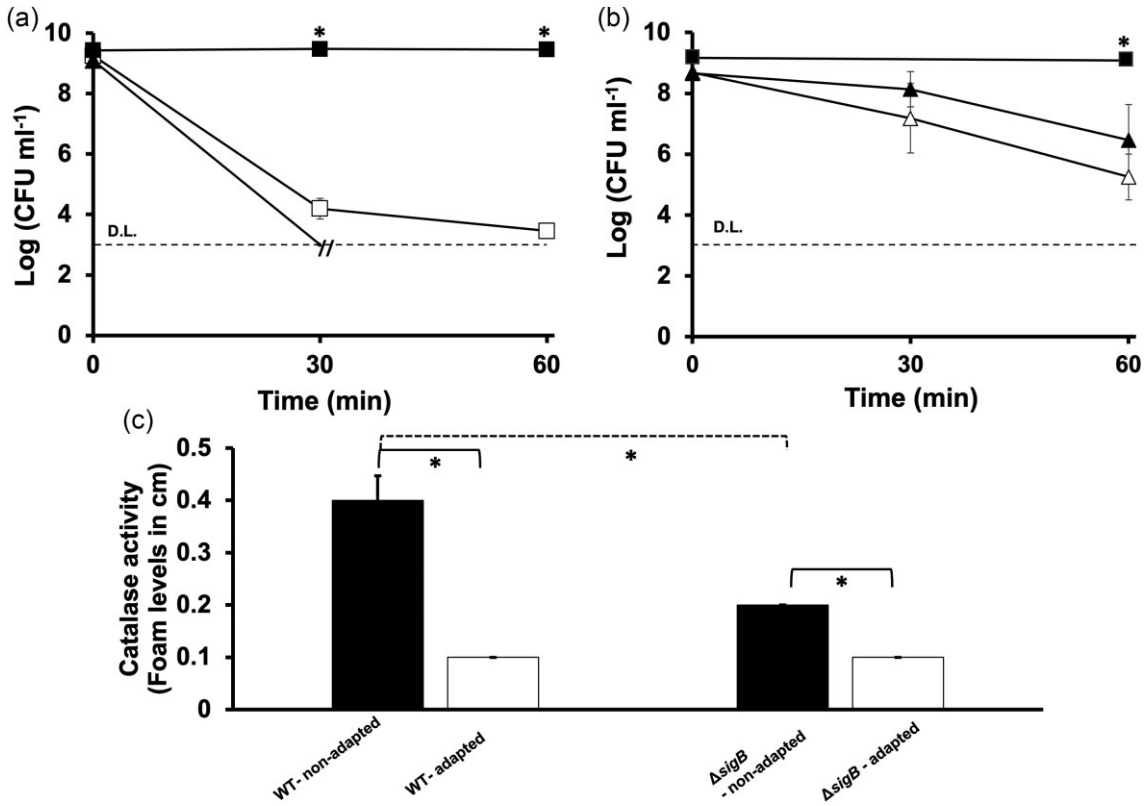

Figure 4. Effect of acid adaptation (HCl) on oxidative stress resistance of exponential phase cultures of *L. monocytogenes* 10403S WT (□/■) and Δ*sigB* (△/▲) with cell transfer from acid adaptation to the lethal H_2O_2 stress (***first approach***). Cultures were grown in BHI broth until the exponential phase, and were either adapted to sublethal acid stress (HCl) at pH 4.5 (□/△) or, left untouched as non-acid-adapted controls (■/▲) for 30 min. They were subsequently harvested, resuspended to fresh BHI (pH 7.2) and WT was challenged with 1.5% H_2O_2 (a), while Δ*sigB* with 0.8% H_2O_2 (b). Catalase activity on the above acid-adapted (white bars), or non-stress-adapted control (black bars) cultures were also investigated after harvesting and resuspension to fresh BHI, but immediately prior to the H_2O_2 challenge (c). D.L. denotes the detection limit of the assay and asterisks denote a statistically significant difference ($P \leq 0.01$). Error bars represent the standard deviation of three independent biological replicates, while each comprised three technical replicates.

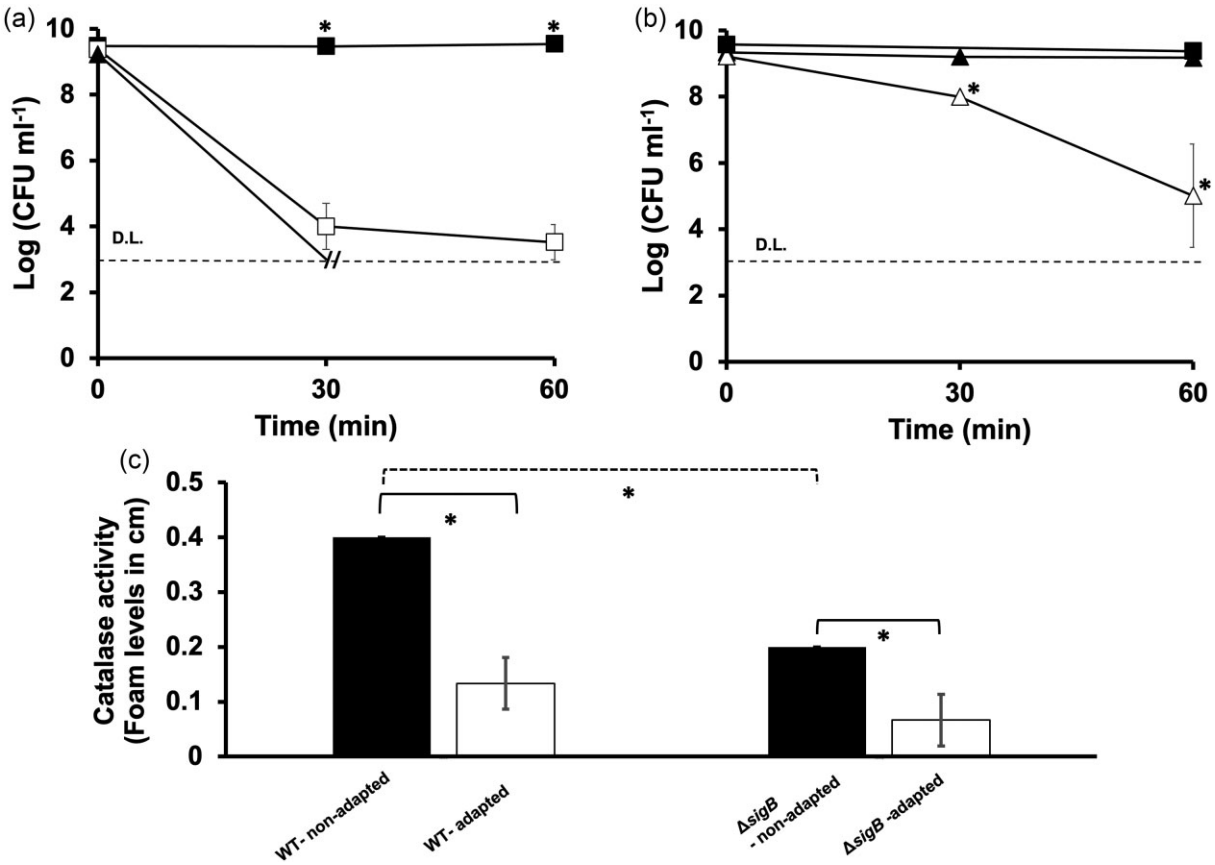

Figure 5. Effect of acid adaptation on oxidative stress resistance of *L. monocytogenes* 10403S WT (□/■) and Δ*sigB* (△/▲) from the exponential phase with the application of H_2O_2 without cell transfer (***second approach***). Cultures were grown until the exponential phase and were either adapted to sublethal acid stress (HCl) at pH 4.5 (□/△) or, left untouched as non-acid-adapted controls for 30 min (■/▲). Subsequently, they were challenged with 0.5% H_2O_2 (a) and 0.35% H_2O_2 (b) without any harvesting or cell transfer step. Catalase activity on the above acid-adapted (white bars) or non-stress-adapted control (black bars) cultures was also investigated immediately prior to the H_2O_2 challenge (c). D.L. denotes the assay's detection limit and asterisks denote a statistically significant difference ($P \leq 0.01$). Error bars represent the standard deviation of three independent biological replicates while each comprised three technical replicates.

maintained (***second approach***; 5.81 log reduction in 60 min; Fig. 5b). Non-adapted WT showed no reduction after 60 min (Fig. 5b) and as such, it was significantly more resistant than Δ*sigB*.

Survival following adaptation to salt and cell transfer to lethal H_2O_2 challenge (*first approach*)

We also assessed the behaviour of cells following adaptation to sublethal levels of salt (0.5 mol l^{-1} NaCl; Abram et al. 2008, Utratna et al. 2011), which is another stress that upregulates *sigB* expression (Utratna et al. 2011). Also, in this case, various H_2O_2 concentrations were tested, and 2.2% and 1.6% H_2O_2 were used for both WT and Δ*sigB*.

Similarly to adaptation to acid, salt adaptation, followed by cell transfer to fresh BHI (***first approach***; pH 7.2), 2.2% H_2O_2 resulted in a sensitive phenotype for WT, as adapted cells showed a significant 5.73 log reduction compared to 0.76 without adaptation to salt (Fig. 6a). Non-adapted Δ*sigB* showed complete inactivation within 20 min (no counts recovered; Fig. 6a) and as such, was more sensitive than the WT.

Furthermore, similarly to acid adaptation experiments, 1 h adaptation to salt followed by cell transfer to lethal 1.6% H_2O_2, did not significantly alter the behaviour of the Δ*sigB* mutant, as both adapted and non-adapted cells showed similar reduction (Fig. 6b). Non-adapted WT showed no reduction after 60 min (Fig. 6b) and as such, it was significantly more resistant than Δ*sigB*.

Survival following adaptation to salt and exposure to lethal H_2O_2 stress with maintenance of the adaptation stress (*second approach*)

We also performed experiments where, following 1 h adaptation to salt, cells were not harvested and H_2O_2 was applied, while the sublethal salt levels were present (***second approach***). Final concentrations of 1.5% and 1.25% H_2O_2 for the WT and Δ*sigB* with the latter being significantly more sensitive to H_2O_2.

Also in the***second approach*** experiments, salt-adapted WT was more sensitive to 1.5% H_2O_2 (2.87 log reduction within 60 min) than its non-salt-adapted control (no cell death observed within 60 min; Fig. 7a). Non-adapted Δ*sigB* showed complete inactivation within 20 min (no counts recovered; Fig. 7a) and as such, was more sensitive than the WT.

However, when salt-adapted Δ*sigB* was challenged with 1.25% H_2O_2 behaved similarly to its non-salt-adapted control (Fig. 7b) and they were both reduced by 5 log CFU ml^{-1}. Non-adapted WT showed no reduction after 60 min (Fig. 7b) and as such, it was significantly more resistant than Δ*sig*.

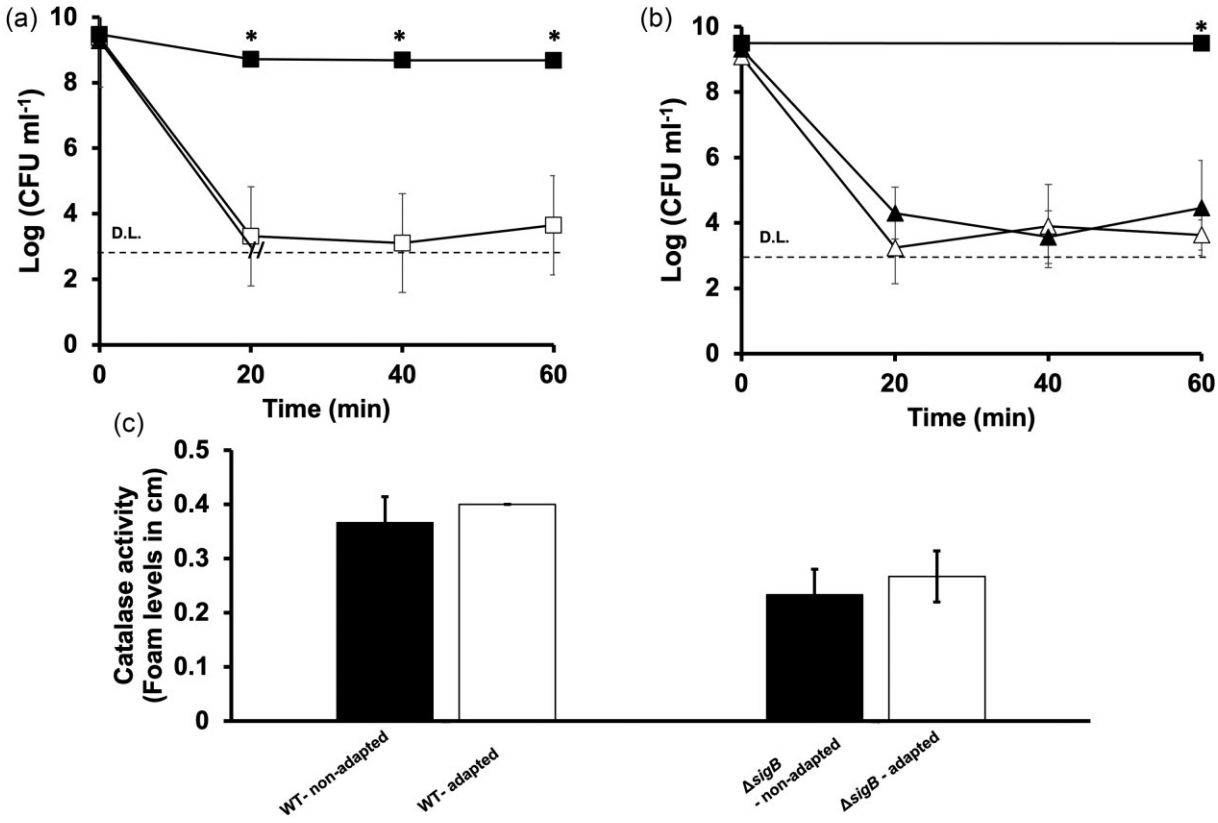

Figure 6. Effect of adaptation to salt on oxidative stress resistance of *L. monocytogenes* 10403S (□/■) and Δ*sigB* (△/▲) from the exponential phase with cell transfer from the salt adaptation to the lethal H_2O_2 stress (***first approach***). Cultures were grown in BHI at 37°C until the exponential phase and were either adapted to 0.5 mol l^{-1} NaCl (□/△) or left untouched as non-salt-adapted controls (■/▲) for 60 min. Subsequently, they were harvested, resuspended in fresh BHI (pH 7.2), and immediately, WT was challenged with 2.2% H_2O_2 (a) and Δ*sigB* with 1.6% H_2O_2 (b). Catalase activity on the above cells adapted to 0.5 mol l^{-1} NaCl (white bars) or control (black bars) was also investigated immediately after the harvesting and resuspension to fresh BHI, but prior to the H_2O_2 challenge (c). D.L. denotes the detection limit of the assay and asterisks denote a statistically significant difference ($P \leq 0.01$). Error bars represent the standard deviation of three independent biological replicates while each comprised three technical replicates.

Catalase activity during survival assays

As in previous work (Boura et al. 2016), it was shown that catalase is a major determinant in oxidative stress resistance, catalase activity was performed in identical duplicate cultures in parallel to all survival assays. A significant reduction in catalase activity was observed in WT and Δ*sigB* after acid adaptation, harvesting, and resuspension to fresh BHI (***first approach***; Fig. 4c; $P < 0.05$). Following acid adaptation, the levels of catalase activity in the WT and Δ*sigB* were similar. It should be mentioned that these catalase activity tests were performed at the point immediately prior to the application of lethal oxidative stress in the experiments presented in Fig. 4a and b but also in those at Fig. 3a and b, including the ultrasound treatment (Fig. 3b).

Similarly, a significant reduction was observed in catalase activity of WT and Δ*sigB* after acid adaptation (***second approach***; Fig. 5c; $P < 0.05$). Interestingly, without acid adaptation, WT had a higher catalase activity than Δ*sigB*, while following acid adaptation, the levels of catalase activity in the WT were comparable to those of the Δ*sigB* (Fig. 5c).

In the experiments with salt adaptation (0.5 mol l^{-1} NaCl) with cell transfer (***first approach***), salt adaptation had no significant impact on catalase levels, neither in WT nor in Δ*sigB* (Fig. 6c). Interestingly, catalase activity of both adapted and non-adapted Δ*sigB* cells was lower than that of the corresponding WT cultures (Fig. 6c). Similarly, in experiments with salt adaptation omitting cell transfer (***second approach***), adaptation to salt, had no significant impact on catalase levels neither in WT nor in Δ*sigB* (Fig. 7c). Also in this case, catalase activity of both adapted and non-adapted Δ*sigB* was lower than that of the corresponding WT cultures (Fig. 7c).

Discussion

Listeria monocytogenes is the deadliest foodborne bacterial pathogen in the UK, the USA, and other countries (FDA/USDA. 2003, Mook et al. 2010). It encounters oxidative stress during decontamination processes (e.g. oxidative disinfectants), novel food processing techniques (plasma treatment and sonication; Spiteri et al. 2017) but also in the phagocytic vacuole of macrophages (Dessaux et al. 2021). *Listeria monocytogenes* possess various oxidative stress resistance mechanisms such as catalase, a scavenger protein, responsible for H_2O_2 detoxification and conversion into less toxic molecules (H_2O and O_2) (Imlay 2003, 2008). Previously, we showed that SigB, the main stress gene regulator in *L. monocytogenes*, that normally protects cells from multiple stresses, makes cells sensitive to oxidative stress. This phenotype was confirmed in two strains (10403S and EGD-e) and occurs during stationary phase under aerobic growth, while it is catalase-mediated (Boura et al. 2016). Therefore, understanding listerial oxidative stress will not only help reduce its presence in foods and food preparation premises, but will also provide a better un-

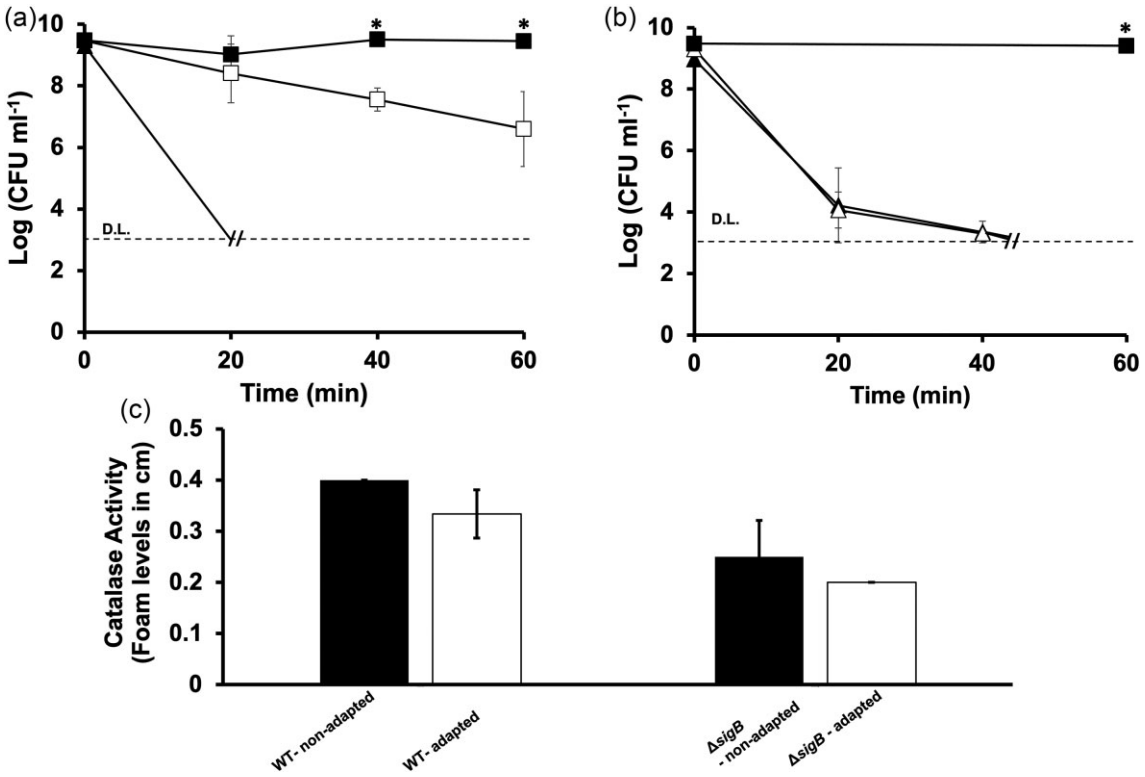

Figure 7. Effect of adaptation to salt on oxidative stress resistance of *L. monocytogenes* 10403S (□/■) and Δ*sigB* (△/▲) from the exponential phase without cell transfer (***second approach***). Cultures grown until the exponential phase were either adapted to 0.5 mol l^{-1} NaCl (□/△) or left untouched (■/▲) for 60 min. Subsequently, they were challenged with 1.5% H_2O_2 (a) or 1.25% H_2O_2 (b) without any harvesting step or transfer to another medium. Catalase activity on the above cells adapted to 0.5 mol l^{-1} NaCl (white bars) or control (black bars) was also investigated immediately prior to the H_2O_2 challenge (c). D.L. denotes the detection limit of the assay and asterisks denote a statistically significant difference ($P \leq 0.01$). Error bars represent the standard deviation of three independent biological replicates while each comprised three technical replicates.

derstanding of its virulence and possibly guide strategies to diminish it.

Since growth phase and SigB are important parameters for oxidative stress resistance and catalase activity in *L. monocytogenes*, we performed a temporal analysis of catalase activity per cell and transcription of the only catalase gene (*kat*), during growth in both 104030S WT and Δ*sigB*. At 4 h of growth (mid-exponential phase), catalase activity per cell (Fig. 1; Boura et al. 2016) and transcription (Fig. 2) were similarly low in WT and Δ*sigB*. All the above explain the previously reported similar oxidative stress resistance between WT and Δ*sigB* at this growth stage (Boura et al. 2016).

At late exponential phase, (∼6 h of growth) catalase activity (Fig. 1), and *kat* transcription (Fig. 2) increased, with the latter showing a peak, which was higher in Δ*sigB* compared to the WT. This higher transcription in Δ*sigB* translated into a higher catalase activity, 2 h later, at 8 h (Fig. 1), when transcription had already dropped in both WT and Δ*sigB*, at similarly low levels (Fig. 2). This delayed increase in catalase activity compared to the transcription, could be explained by a possible intracellular catalase accumulation through time. However, at 6 h, catalase activity seems to be variable as seen by the higher standard deviation, implying a major change in catalase transcription and catalase activity. The higher catalase activity of Δ*sigB* compared to WT at 8 h of growth and beyond (Fig. 1) explains its previously observed higher oxidative stress resistance (Boura et al. 2016). Following its drop at 8 h, catalase transcription, remained at similarly low levels until 10 h in both WT and Δ*sigB* (Fig. 2). We did not look at transcription beyond 10 h, as no difference occurred in catalase activity beyond 8 h (Fig. 1). However, no difference in *kat* transcription was previously found between WT and Δ*sigB* at 18 h (Boura et al. 2016) and 8 and 16 h of growth (EGD-e; Hain et al. 2008).

The SigB-mediated downregulation of *kat* at 6 h of growth is puzzling since no consensus SigB box is present upstream of *kat* (Hain et al. 2008), while SigB does not normally act as a repressor, but as a transcriptional activator, by binding to the core RNA polymerase (Kazmierczak et al. 2005). Interestingly, a similar behaviour of higher catalase activity and hyperresistance to oxidative stress in Δ*sigB* has also been observed in *B. subtilis* (van Schaik et al. 2005). A possible explanation for the above phenomena could be associated with SigB promoting expression of PerR, a repressor of peroxide-inducible genes (e.g. catalases) in Gram-positive bacteria (Fuangthong et al. 2002, Faulkner et al. 2012, Seixas et al. 2025). Loss of *sigB* could result in lower PerR activity leading to *kat* upregulation (Herbig and Helmann 2001, Horsburgh et al. 2001, Rea et al. 2004, Faulkner et al. 2012, Seixas et al. 2025), although this still needs to be demonstrated in *L. monocytogenes*. Another possible explanation could be that *kat* is being upregulated in Δ*sigB*, to counteract for the loss of another oxidative stress resistance mechanism such as SpxA, which upregulates catalase under aerobic conditions (Cesinger et al. 2020) and requires SigB for its expression (Gaballa et al. 2019).

Since cells in the environment are normally exposed to multiple stresses, we decided to look at the effect of stress adaptation on oxidative stress and the role of SigB in this context.

First, we looked at the effect of acid adaptation on oxidative stress and as it has been shown previously (Dhowlaghar et al. 2019), acid adaptation significantly enhanced sensitivity to oxidative stress during the ***first approach*** (Fig. 3a). Furthermore, we investigated if the observed effect of acid adaptation occurs when another oxidative stress-based technology such as ultrasound (Spiteri et al. 2017) is used. Indeed, as in the case of H_2O_2, acid adaptation enhanced sensitivity to ultrasound, resulting in a synergistic effect even after the removal of the acid stress (Fig. 3b).

The case of increased sensitivity towards oxidative stress following adaptation to mild sublethal acidic conditions is rare as normally adaptation to one stress results in protection against other stresses (Lou and Yousef 1997, Ferreira et al. 2003, Sue et al. 2004, Wemekamp-Kamphuis et al. 2004) and not increased sensitivity as shown here. Cross-protection between stresses is normally mediated by SigB (O'Byrne and Karatzas 2008), although we have shown previously that SigB can have the opposite effect, by reducing the oxidative stress resistance of aerobically grown stationary phase *L. monocytogenes* (Boura et al. 2016). Therefore, by employing an isogenic *sigB* deletion mutant, we decided to investigate the role of SigB in oxidative stress following stress adaptation.

Following acid adaptation of WT under conditions (pH 4.5) that are known to upregulate *sigB* (Chaturongakul and Boor 2006, Ondrusch and Kreft 2011, Utratna et al. 2014) and challenge with H_2O_2, we observed a 6 log reduction, while non-adapted WT cells remained largely unaffected (Fig. 4a). On the other hand, acid adaptation at pH 4.5 did not affect the oxidative stress resistance in Δ*sigB* to the non-adapted Δ*sigB* control (Fig. 4b). Therefore, this hypersensitivity to oxidative stress occurs only in the presence of SigB (WT) and not in its absence (Δ*sigB*), underpinning a SigB-mediated phenomenon.

We thought that this hypersensitivity to oxidative stress could be the result of sublethal injury or induction of a viable but nonculturable (VBNC) state caused by the acid adaptation step. However, VBNC state is not likely as the adaptation conditions did not affect viability. Furthermore, conditions were within the growth range of this particular strain (Abram et al. 2008, Cheng et al. 2015) resulting in robust cells with increased multiple stress resistance (Lou and Yousef 1997, Ferreira et al. 2003, Sue et al. 2004, Wemekamp-Kamphuis et al. 2004). In addition, the acid-adapted Δ*sigB* and the non-adapted control showed similar oxidative stress resistance (Fig. 4b), suggesting no negative impact of acid adaptation on oxidative stress resistance and therefore, no sublethal injury. Since acid adaptation caused no sublethal injury to Δ*sigB*, the same is valid for the significantly more robust WT, suggesting no role for the sublethal injury.

We previously associated the hypersensitivity of WT to oxidative stress at stationary phase with catalase activity (Boura et al. 2016). Therefore, we looked at catalase activity to explain the above results. We found that acid adaptation significantly reduced catalase activity in WT (Fig. 4c), and this could explain the hypersensitivity to oxidative stress following acid adaptation (Fig. 4a). On the other hand, the effect of acid adaptation on the catalase activity of Δ*sigB* was much lower, and of significantly lower magnitude compared to the WT (Fig. 4c). This could largely explain the minor non-statistically significant reduction in the oxidative stress resistance of Δ*sigB*, following acid adaptation (Fig. 4b). Overall, the catalase activity results (Fig. 4c) largely explain the oxidative stress resistance of acid-adapted WT (Fig. 4a) and Δ*sigB* (Fig. 4b). As there is a variety of oxidative stress mechanisms that might be upregulated by SigB, a minor discrepancy between oxidative stress resistance (Fig. 4b) and catalase activity (Fig. 4c), as this one seen in Δ*sigB*, is expected. Our results also link previous oxidative stress hypersensitivity observed by Dhowlaghar et al. (2019) and Boura et al. (2016) with SigB upregulation.

In addition, we followed a ***second approach*** , with omitting the harvesting and resuspension of cells in fresh BHI broth, thereby exposing cells to both the adaptation stresses (acid) and the lethal stress (H_2O_2) coinciding. Similarly to the ***first approach***, acid-adapted WT was more sensitive to oxidative stress than its non-acid-adapted control (Fig. 5a). This clearly indicates an important synergistic effect between acidic conditions and H_2O_2, which according to our knowledge, has not been shown before in such a setup. Jyung et al. (2023) have previously shown a synergistic effect between plasma-activated water and lactic, malic acid, citric acid, and acetic acid, whereas propionic acid did not show any synergistic effect. However, HCl was not assessed, and the setup did not involve any adaptation step. In the ***second approach***, when we employed Δ*sigB* (Fig. 5b), similarly to the WT, the results suggest that the role of SigB in this challenge was relatively limited. This was expected since both adaptation acid stress and the lethal oxidative stress coincided, and the survival depended on a variety of mechanisms and not solely on oxidative stress mechanisms such as catalase. This is obvious since, to achieve a comparable inactivation in the ***fi r st approach***, we used 1.5% and 0.8% H_2O_2 for the WT and Δ*sigB* (Fig. 4a and b), while in the ***second approach***, we used 3 times lower H_2O_2 concentrations (Fig. 5a and b). Also, in these experiments, catalase activity was reduced by the acid adaptation step in both WT and Δ*sigB* (Fig. 5c), explaining the lower survival of both strains in the coinciding stress application (Fig. 5a and b). We also observed that the catalase activity of WT and Δ*sigB* was not affected by harvesting and resuspension in fresh BHI (comparison between Fig. 4c and Fig. 5c).

We also investigated the effects of salt adaptation on oxidative stress resistance. Similarly to experiments with acid adaptation (Fig. 4a), salt-adapted WT (0.5 mol l^{-1} NaCl), in the ***first approach***, was more sensitive to oxidative stress compared to the non-adapted control (Fig. 6a). Similarly to the case with acid adaptation, the results here signify a very interesting synergistic effect between salt adaptation and H_2O_2, although the salt stress was removed and not present during the subsequent oxidative stress.

Furthermore, similarly to acid adaptation (Fig. 4b), adaptation to 0.5 mol l^{-1} NaCl did not alter the oxidative stress resistance of Δ*sigB* (Fig. 6b). Therefore, since this hypersensitivity to oxidative stress occurred only in the presence of SigB (WT) and not in its absence (Δ*sigB*), we could assume that it is a SigB-mediated phenomenon. Interestingly, this effect was not catalase-mediated, as catalase activity remained unchanged prior to and post-salt adaptation (Fig. 6c). These results are novel, and they are also in contrast to the concept of cross-protection between different stresses, showing that salt adaptation enhances sensitivity to oxidative stress. In addition, all results together confirm a general pattern, where *sigB* upregulation enhances sensitivity to oxidative stress.

The ***second approach*** was also used with salt adaptation. Results for the WT were similar to those obtained with the ***first approach*** (Fig. 5a), as salt adaptation increased the sen-

sitivity of WT to oxidative stress (Fig. 7a), but not that of Δ*sigB* (Fig. 7b). The latter behaviour of Δ*sigB* differs from that with acid adaptation (Fig. 5b). This suggests that in the case of salt adaptation stress coinciding with the lethal oxidative stress, the effect was SigB-mediated. Also in this case, and in contrast to acid adaptation experiments (Figs 4c and 5c), salt adaptation had no noticeable effect on catalase activity (Figs 6c and 7c), and the effects observed are probably attributed to other oxidative stress mechanisms. A possible explanation might be associated with the downregulation of 2-cys peroxiredoxin (*lmo1604*), by SigB in the presence of salt (Abram et al. 2008). In previous work, Yadav et al. (2019) showed that salt concentration did not affect the inactivation of *L. innocua* during cold plasma treatment of ham. However, our results explain the previously-observed increased inactivation of *L. monocytogenes* in high salt level cheese brines following a challenge with 100-ppm H_2O_2 (Glass et al. 2024).

Similarly to the acid adaptation experiments, salt-adapted cells were more sensitive during the ***second approach*** (Fig. 7a and b) than those at the ***first approach*** (Fig. 6a and b) since lower H_2O_2 levels were used for the latter to achieve a lethal effect. In all the above experiments, we included controls without stress adaptation, and we found that controls of Δ*sigB* were significantly more sensitive to oxidative stress than WT, when challenged with similar H_2O_2 concentrations. This could be explained at least partly by the consistently higher catalase activity of WT compared to Δ*sigB* in the exponential phase as seen in Figs 4c, 5c, 6c, and 7c. This difference in catalase activity was accompanied by a statistical significance in Figs 4c and 5c (5.5 h of growth), but not in Figs 6c and 7c (6 h of growth). It should be stated here that survival and catalase activity measurements were not performed at 5 h of growth but after the adaptation step was completed, at 5.5 and 6 h for acid- and the salt-adapted including their non-stress-adapted controls respectively. Beyond this point, and into stationary phase, catalase activity in Δ*sigB* remains higher than that of WT (Fig. 1) and clearly results in the higher oxidative stress resistance documented previously (Boura et al. 2016).

The higher sensitivity of Δ*sigB* compared to the WT at 5.5–6 h of growth, might counteract the argument that the presence of *sigB* increases sensitivity to H_2O_2. However, the main point in the present work was to look at the role of SigB, following acid and salt adaptation. It could be concluded that, during the exponential phase, *sigB* transcription is relatively low (Utratna et al. 2011, 2012, 2014), which however might lead to a low-level induction of multiple mechanisms, protecting against oxidative stress. However, once exponential phase cells are exposed to mild acidic conditions similar to those used by various studies previously (Chaturongakul and Boor 2006, Ferreira et al. 2001, Sue et al. 2004, Wemekamp-Kamphuis et al. 2004), or mild osmotic conditions (Abram et al. 2008, Ferreira et al. 2001, Kazmierczak et al. 2003, Utratna et al. 2012, 2014), *sigB* transcriptional upregulation occurs. The latter, although protects cells against multiple stresses, it makes them sensitive to oxidative stress.

The above results are novel and give a further insight into the oxidative stress resistance of *L. monocytogenes* and the negative role of SigB. It should be mentioned that Lou and Yousef (1997) have shown that adaptation to 7% NaCl or acid (HCl; pH 4.5) enhances oxidative stress resistance in *L. monocytogenes* ScottA. However, their work was performed with Scott A, while ours with 10403S. We have confirmed these findings with EGD-e as well (data not shown). Furthermore, the above authors performed their survival assays in PB, or saline buffer at 4°C, resulting in a cold shock and subsequently transferred cells to 30°C, while their survival assays lasted for 8 h, with low H_2O_2 concentrations (0.1%). Such long exposures could allow the deployment of various additional oxidative stress resistance mechanisms, which could explain this discrepancy. In our case, we applied significantly higher H_2O_2 concentrations, not allowing any cellular responses. In other work, it has also been shown that adaptation to salt leads to increased *kat* transcription and oxidative stress resistance (Bergholz et al. 2012); however, in that case, cells were grown without aeration. Lack of aeration results in a dramatically different behaviour in *L. monocytogenes*, with SigB not playing a role or in some cases protecting against oxidative stress, while under aeration, it has the opposite effect (Boura et al. 2016). As mentioned above, our work here agrees with and explains the work of Dhowlaghar et al. (2019), Jyung et al. (2023), Glass et al. (2024), and Boura et al. (2016), although further work is required to identify the mechanism(s) through which SigB downregulates or inhibits the activity of oxidative stress mechanisms such as catalase.

Oxidative stress plays a role in listerial virulence, as it is one of the main mechanisms of bacterial inactivation in the phagolysosome (Flannagan et al. 2015, Herb and Schramm 2021). The role of SigB in virulence is clear in the initial stages of invasion facilitating the upregulation of internalins, and LLO (Boura et al. 2016, Dessaux et al. 2021). However, its role in proliferation, and later stages of the virulence cycle and particularly survival in the phagolysosome is not clear. Some lines of research show that SigB plays no role in proliferation and survival in the phagolysosome, since Δ*sigB* proliferates at a similar rate as the WT (Kim et al. 2004, Soraya et al. 2011, Boura et al. 2016) or even higher (Rukit et al. 2022). In addition, *sigB* is not significantly upregulated intracellularly (Chatterjee et al. 2006, Boura et al. 2016), supporting the latter concept, as *sigB* upregulation in the phagolysosome would result in high sensitivity to its acidic and oxidative stress conditions (Uribe-Querol and Rosales 2017, Santiago-Burgos et al. 2022). On the other hand, another line of research shows that SigB plays a role in intracellular proliferation as oxidative stress in the phagocytic vacuole upregulates Prli42, that activates RsbR1, which, in turn, activates SigB and tethers the stresso`some to the listerial membrane (Dessaux et al. 2021). However, the stressosome core protein remains undetectable intracellularly raising the question of how the stressosome can function without its core protein (Impens et al. 2017). It is possible that the key is the level of SigB upregulation that might be subject to fine-tuning. For example, during exponential phase, low levels of *sigB* transcription upregulate various background mechanisms (e.g. removal of denatured proteins), providing a survival advantage to the WT over Δ*sigB* (Figs 5c and 7c). However, high level of *sigB* upregulation, could reduce catalase activity, or the expression of other oxidative stress mechanisms providing a survival advantage to Δ*sigB*. Therefore, more work is required to clarify the above phenomena.

Overall, the present study provides further insight into the activity and transcription of catalase at different growth stages of *L. monocytogenes*. It also enhances our knowledge of the role of acid and salt adaptation in oxidative and ultrasound stress resistance, in association with SigB and catalase activity. We demonstrate that adaptation to mild acid or salt stress

acts synergistically with oxidative stress even if the adaptation stresses are removed. This complements the well-known concept of cross protection (O'Byrne and Karatzas 2008, Bergholz et al. 2012) between stresses, which does not seem to be applicable with oxidative stress. As this phenomenon of cross protection between stresses is normally associated with SigB, we also show that the above phenomena are also attributed to SigB, where the latter, instead of protecting, it enhances sensitivity to oxidative stress. By taking advantage of these synergistic effects, we could possibly use oxidative stress-based technologies in combination with acid or salt, to efficiently eliminate *L. monocytogenes* or enhance the efficacy of the oxidative stress-based technologies. It should be stated that such technologies (e.g. ultrasound, or plasma etc.) have limited penetration in the food industry (dos Santos Rocha et al. 2022) due to their low efficacy. The above observations could enhance the antimicrobial effects of these technologies, optimize their application, or enhance their efficacy in combination with other stresses, making them more effective for use in food safety. They also contribute to our deeper understanding of the intracellular cycle of *L. monocytogenes*.

Acknowledgements

We thank all members of the FMSU and colleagues in the Department of Food and Nutritional Sciences, University of Reading, Reading, United Kingdom for helpful discussions. The *sigB* mutant strain used in this study was generously supplied by Kathryn Boor (Cornell University), Cormac Gahan (University College Cork), and Conor P. O'Byrne (NUI Galway, Ireland).

Author contributions

Marcia Boura (Data curation, Investigation, Methodology, Writing - original draft), Mahide Muge Yilmaz Topcam (Data curation, Investigation, Methodology, Writing - original draft, Writing - original draft), David Spiteri (Data curation, Investigation, Methodology, Writing - original draft), Carolina Bruschi Silva (Investigation, Methodology, Writing - original draft), Vasileios Valdramidis (Conceptualization, Resources, Supervision, Writing - review & editing), and Kimon Andreas G. Karatzas (Conceptualization, Funding acquisition, Methodology, Project administration, Resources, Supervision, Writing - review & editing)

Conflict of interest: None declared.

Funding

M.B. was supported by a Marie Curie European Reintegration Grant (grant ERG 265154) awarded to K.A.G.K., and funds from the University of Reading. M.M.Y.T. was supported by doctoral studies grant from the Ministry of National Education (YLSY), Republic of Turkey. C.B. was supported by a CAPES—Brazil grant (No. 99999.0022146/2015–00).

Data availability

The data presented in this article will be shared upon request to the corresponding author.

References

Abram F, Starr E, Karatzas KAG *et al*. Identification of components of the SigB regulon in *Listeria monocytogenes* that contribute to acid and salt tolerance. *Appl Environ Microb* 2008;**74**:6848–58. https://doi.org/10.1128/aem.00442-08

Baranyi J, Roberts TA. A dynamic approach to predicting bacterial growth in food. *Int J Food Microbiol* 1994;**23**:277–94. https://doi.org/10.1016/0168-1605(94)90157-0

Baranyi J, Ross T, McMeekin TA *et al*. Effects of parameterization on the performance of empirical models used in `predictive microbiology'. *Food Microbiol* 1996;**13**:83–91. https://doi.org/https://doi.org/10.1006/fmic.1996.0011

Bergholz TM, Bowen B, Wiedmann M *et al*. *Listeria monocytogenes* shows temperature-dependent and -independent responses to salt stress, including responses that induce cross-protection against other stresses. *Appl Environ Microb* 2012;**78**:2602–12. https://doi.org/10.1128/AEM.07658-11

Bonnet M, Montville TJ. Acid-tolerant *Listeria monocytogenes* persist in a model food system fermented with nisin-producing bacteria. *Lett Appl Microbiol* 2005;**40**:237–42. https://doi.org/10.1111/j.1472-765X.2005.01661.x

Boura M, Keating C, Royet K *et al*. Loss of SigB in *Listeria monocytogenes* strains EGD-e and 10403S confers hyperresistance to hydrogen peroxide in stationary phase under aerobic conditions. *Appl Environ Microb* 2016;**82**:4584–91. https://doi.org/10.1128/AEM.00709-16

Cesinger MR, Thomason MK, Edrozo MB *et al*. *Listeria monocytogenes* SpxA1 is a global regulator required to activate genes encoding catalase and heme biosynthesis enzymes for aerobic growth. *Mol Microbiol* 2020;**114**:230–43. https://doi.org/10.1111/mmi.14508

Chatterjee SS, Hossain H, Otten S *et al*. Intracellular gene expression profile of *Listeria monocytogenes*. *Infect Immun* 2006;**74**:1323–38. https://doi.org/10.1128/IAI.74.2.1323-1338.2006

Chaturongakul S, Boor KJ. Sigma B activation under environmental and energy stress conditions in *Listeria monocytogenes*. *Appl Environ Microb* 2006;**72**:5197–203. https://doi.org/10.1128/AEM.03058-05

Cheng C, Yang Y, Dong Z *et al*. *Listeria monocytogenes* varies among strains to maintain intracellular pH homeostasis under stresses by different acids as analyzed by a high-throughput microplate-based fluorometry. *Front Microbiol* 2015;**6**:15. https://doi.org/10.3389/fmicb.2015.00015

Cortes, B.W., Naditz, A.L., Anast, J.M., Schmitz-Esser, S.. Transcriptome Sequencing of Listeria monocytogenes Reveals Major Gene Expression Changes in Response to Lactic Acid Stress Exposure but a Less Pronounced Response to Oxidative Stress. *Front Microbiol*. 2020;**10**:3110. doi: 10.3389/fmicb.2019.03110. .

Davidson PM, Harrison MA. Resistance and adaptation to food antimicrobials, sanitizers, and other process controls. *Food Technol* 2002;**56**:69–78.

Dessaux C, Pucciarelli MG, Guerreiro DN *et al*.. Activation of the *Listeria monocytogenes* stressosome in the intracellular eukaryotic environment. *Appl Environ Microb* 2021;**87**:e00397–21. https://doi.org/10.1128/AEM.00397-21

Dhowlaghar N, Shen Q, Nannapaneni R *et al*. Survival of acid stress adapted cells of *Listeria monocytogenes* serotypes 1/2a and 4b in commonly used disinfectants in broth and water models. *LWT* 2019;**109**:201–6. https://doi.org/https://doi.org/10.1016/j.lwt.2019.04.007

dos Santos Rocha C, Magnani M, de Paiva Anciens Ramos GL *et al*. Emerging technologies in food processing: impacts on sensory characteristics and consumer perception. *Curr Opin Food Sci* 2022;**47**:100892. https://doi.org/https://doi.org/10.1016/j.cofs.2022.100892

Faulkner MJ, Ma Z, Fuangthong M *et al*. Derepression of the *Bacillus subtilis* PerR peroxide stress response leads to iron deficiency. *J Bacteriol* 2012;**194**:1226–35. https://doi.org/10.1128/JB.06566-11

FDA/USDA. No Title. Docket No. 1999N-1168. 68. 2003.

Ferreira A, Gray M, Wiedmann M *et al*. Comparative genomic analysis

of the sigB operon in *Listeria monocytogenes* and in other gram-positive bacteria. *Curr Microbiol* 2004;**48**:39–46. https://doi.org/10.1007/s00284-003-4020-x

Ferreira A, O'Byrne CP, Boor KJ. Role of σ^B in heat, ethanol, acid, and oxidative stress resistance and during carbon starvation in *Listeria monocytogenes*. *Appl Environ Microb* 2001;**67**:4454–7. https://doi.org/10.1128/aem.67.10.4454-4457.2001

Ferreira A, Sue D, O'Byrne CP *et al*. Role of *Listeria monocytogenes* σ^B in survival of lethal acidic conditions and in the acquired acid tolerance response. *Appl Environ Microb* 2003;**69**:2692–8https://doi.org/10.1128/AEM.69.5.2692-2698.2003

Flannagan RS, Heit B, Heinrichs DE. Antimicrobial mechanisms of macrophages and the immune evasion strategies of *Staphylococcus aureus*. *Pathogens* 2015;**4**:826–68. https://doi.org/10.3390/pathogens4040826

Fuangthong M, Herbig AF, Bsat N *et al*. Regulation of the *Bacillus subtilis fur* and *perR* genes by PerR: not all members of the PerR regulon are peroxide inducible. *J Bacteriol* 2002;**184**:3276–86. https://doi.org/10.1128/JB.184.12.3276-3286.2002

Gaballa A, Guariglia-Oropeza V, Wiedmann M *et al*. Cross talk between SigB and PrfA in *Listeria monocytogenes* facilitates transitions between extra- and intracellular environments. *Microbiol Mol Biol Rev* 2019;**83**. https://doi.org/10.1128/MMBR.00034-19

Glass KA, Lim JY, Singer QL. Inactivation of *Listeria monocytogenes* by hydrogen peroxide addition in commercial cheese brines. *J Food Prot* 2024;**87**:100191. https://doi.org/10.1016/j.jfp.2023.100191

Hain T, Hossain H, Chatterjee SS *et al*. Temporal transcriptomic analysis of the *Listeria monocytogenes* EGD-e sigma B regulon. *BMC Microbiol* 2008;**8**:20. https://doi.org/10.1186/1471-2180-8-20

Heisick JE, Wagner DE, Nierman ML *et al*. *Listeria* spp. Found on fresh market produce. *Appl Environ Microb* 1989;**55**:1925–7. https://doi.org/10.1128/aem.55.8.1925-1927.1989

Herb M, Schramm M. Functions of ROS in macrophages and antimicrobial immunity. *Antioxidants* 2021;**10**:313. https://doi.org/10.3390/antiox10020313

Herbig AF, Helmann JD. Roles of metal ions and hydrogen peroxide in modulating the interaction of the *Bacillus subtilis* PerR peroxide regulon repressor with operator DNA. *Mol Microbiol* 2001;**41**:849–59. https://doi.org/10.1046/j.1365-2958.2001.02543.x

Horsburgh MJ, Clements MO, Crossley H *et al*. PerR controls oxidative stress resistance and iron storage proteins and is required for virulence in *Staphylococcus aureus*. *Infect Immun* 2001;**69**:3744–54. https://doi.org/10.1128/IAI.69.6.3744-3754.2001

Imlay JA. Cellular defenses against superoxide and hydrogen peroxide. *Annu Rev Biochem* 2008;**77**:755–76. https://doi.org/10.1146/annurev.biochem.77.061606.161055

Imlay JA. Pathways of oxidative damage. *Annu Rev Microbiol* 2003;**57**:395–418. https://doi.org/10.1146/annurev.micro.57.030502.090938

Impens F, Rolhion N, Radoshevich L *et al*. N-terminomics identifies Prli42 as a membrane miniprotein conserved in firmicutes and critical for stressosome activation in *Listeria monocytogenes*. *Nat Microbiol* 2017;**2**:17005. https://doi.org/10.1038/nmicrobiol.2017.5

Iwase T, Tajima A, Sugimoto S *et al*. A simple assay for measuring catalase activity: a visual approach. *Sci Rep* 2013;**3**:3081. https://doi.org/10.1038/srep03081

Jyung S, Kang J-W, Kang D-H. Inactivation of *Listeria monocytogenes* through the synergistic interaction between plasma-activated water and organic acid. *Food Res Int* 2023;**167**:112687. https://doi.org/https://doi.org/10.1016/j.foodres.2023.112687

Karatzas K-AG, Brennan O, Heavin S *et al*. Intracellular accumulation of high levels of γ-aminobutyrate by *Listeria monocytogenes* 10403S in response to low pH: uncoupling of γ-aminobutyrate synthesis from efflux in a chemically defined medium. *Appl Environ Microb* 2010;**76**:3529–37. https://doi.org/10.1128/aem.03063-09

Kazmierczak MJ, Mithoe SC, Boor KJ *et al*. *Listeria monocytogenes* σ^B regulates stress response and virulence functions. *J Bacteriol* 2003;**185**:5722–34. https://doi.org/10.1128/jb.185.19.5722-5734.2003

Kazmierczak MJ, Wiedmann M, Boor KJ. Alternative sigma factors and their roles in bacterial virulence. *Microbiol Mol Biol Rev* 2005;**69**:527–43. https://doi.org/10.1128/MMBR.69.4.527-543.2005

Kim H, Boor KJ, Marquis H. *Listeria monocytogenes* sigma B contributes to invasion of human intestinal epithelial cells. *Infect Immun* 2004;**72**:7374–8. https://doi.org/10.1128/IAI.72.12.7374-7378.2004

Lou Y, Yousef AE. Adaptation to sublethal environmental stresses protects *Listeria monocytogenes* against lethal preservation factors. *Appl Environ Microb* 1997;**63**:1252–5. https://doi.org/10.1128/aem.63.4.1252-1255.1997

Mason TJ. Advances in sonochemistry. *Advances in Sonochemistry*. Elsevier Science, 1999. https://doi.org/10.1093/hesc/9780198503712.001.0001

McLaughlin HP, Hill C, Gahan CG. The impact of iron on *Listeria monocytogenes*; inside and outside the host. *Curr Opin Biotechnol* 2011;**22**:194–9. https://doi.org/10.1016/j.copbio.2010.10.005

Mook P, Grant KA, Little CL *et al*. Emergence of pregnancy-related listeriosis amongst ethnic minorities in England and Wales. *Euro Surveill* 2010;**15**:19610. https://doi.org/10.2807/ese.15.27.19610-en

Moorhead SM, Dykes GA. The role of the *sigB* gene in the general stress response of *Listeria monocytogenes* varies between a strain of serotype 1/2a and a strain of serotype 4c. *Curr Microbiol* 2003;**46**:461–6. https://doi.org/10.1007/s00284-002-3867-6

O'Byrne CP, Karatzas KAG., 2008. Chapter 5 the role of Sigma B (SigB) in the stress adaptations of *Listeria monocytogenes*: overlaps between stress adaptation and virulence. In: Laskin A I., Sariaslani Geoffrey S, Gadd M. (eds.), *Advances in Applied Microbiology*. Academic Press, 115–40.

Oliver HF, Orsi RH, Wiedmann M *et al*. *Listeria monocytogenes* SigB has a small core regulon and a conserved role in virulence but makes differential contributions to stress tolerance across a diverse collection of strains. *Appl Env Microbiol* 2010;**76**:4216–32. https://doi.org/10.1128/AEM.00031–10. Epub 2010 May.

Oliver HF, Orsi RH, Wiedmann M *et al*. Sigma B plays a limited role in the ability of *Listeria monocytogenes* strain F2365 to survive oxidative and acid stress and in its virulence characteristics. *J Food Prot* 2013;**76**:2079–86. https://doi.org/10.4315/0362-028X.JFP-12-542

Ondrusch N, Kreft J. Blue and red light modulates SigB-dependent gene transcription, swimming motility and invasiveness in *Listeria monocytogenes*. *PLoS One* 2011;**6**:e16151. https://doi.org/10.1371/journal.pone.0016151

Quereda JJ, Morón-García A, Palacios-Gorba C *et al*. Pathogenicity and virulence of *Listeria monocytogenes*: a trip from environmental to medical microbiology. *Virulence* 2021;**12**:2509–45. https://doi.org/10.1080/21505594.2021.1975526

Ramaswamy V, Cresence VM, Rejitha JS *et al*. *Listeria*—review of epidemiology and pathogenesis. *J Microbiol Immunol Infect* 2007;**40**:4–13.

Rea RB, Gahan CGM, Hill C. Disruption of putative regulatory loci in *Listeria monocytogenes* demonstrates a significant role for Fur and PerR in virulence. *Infect Immun* 2004;**72**:717–27. https://doi.org/10.1128/iai.72.2.717-727.2004

Rukit J, Boonmee A, Kijpornyongpan T *et al*. Roles of alternative Sigma factors in invasion and growth characteristics of *Listeria monocytogenes* 10403S into Human epithelial colorectal adenocarcinoma caco-2 cell. *Front Microbiol* 2022;**13**. https://doi.org/10.3389/fmicb.2022.901484

Santiago-Burgos EJ, Stuckey PV, Santiago-Tirado FH. Real-time visualization of phagosomal pH manipulation by *Cryptococcus neoformans* in an immune signal-dependent way. *Front Cell Infect Microbiol* 2022;**12**. https://doi.org/10.3389/fcimb.2022.967486

Schultze T, Hilker R, Mannala GK *et al*. A detailed view of the intracellular transcriptome of *Listeria monocytogenes* in murine

macrophages using RNA-seq. *Front Microbiol* 2015;**6**:1199. https://doi.org/10.3389/fmicb.2015.01199

Seixas AF, Silva AFQ, Sousa JP *et al*. The RNA chaperone hfq is a novel regulator of catalase expression and hydrogen peroxide-induced oxidative stress response in *Listeria monocytogenes* EGD-e. *Free Radical Biol Med* 2025;**227**:103–16. https://doi.org/10.1016/j.freeradbiomed.2024.11.038

Shen Q, Soni KA, Nannapaneni R. Stability of sublethal acid stress adaptation and induced cross protection against lauric arginate in *Listeria monocytogenes*. *Int J Food Microbiol* 2015;**203**:49–54. https://doi.org/10.1016/j.ijfoodmicro.2015.02.027

Skandamis PN, Gounadaki AS, Geornaras I *et al*. Adaptive acid tolerance response of *Listeria monocytogenes* strains under planktonic and immobilized growth conditions. *Int J Food Microbiol* 2012;**159**:160–6. https://doi.org/https://doi.org/10.1016/j.ijfoodmicro.2012.07.027

Soraya C, Sarita R, Elizabeth PM *et al*. Transcriptomic and phenotypic analyses identify coregulated, overlapping regulons among PrfA, CtsR, HrcA, and the alternative Sigma factors σ^B, σ^C, σ^H, and σ^L in *Listeria monocytogenes*. *Appl Environ Microb* 2011;**77**:187–200. https://doi.org/10.1128/AEM.00952-10

Spiteri D, Chot-Plassot C, Sclear J *et al*. Ultrasound processing of liquid system(s) and its antimicrobial mechanism of action. *Lett Appl Microbiol* 2017;**65**:313–8. https://doi.org/10.1111/lam.12776

Sue D, Fink D, Wiedmann M *et al*. SigB-dependent gene induction and expression in *Listeria monocytogenes* during osmotic and acid stress conditions simulating the intestinal environment. *Microbiology* 2004;**150**:3843–55. https://doi.org/10.1099/mic.0.27257-0

Uribe-Querol E, Rosales C. Control of phagocytosis by microbial pathogens. *Front Immunol* 2017;**8**:1368. https://doi.org/10.3389/fimmu.2017.01368

Utratna M, Cosgrave E, Baustian C *et al*. Development and optimization of an EGFP-based reporter for measuring the general stress response in *Listeria monocytogenes*. *Bioengineered* 2012;**3**:93–103. https://doi.org/10.4161/bbug.19476

Utratna M, Cosgrave E, Baustian C *et al*. Effects of growth phase and temperature on Sigma B activity within a *Listeria monocytogenes* population: evidence for RsbV-independent activation of Sigma B at refrigeration temperatures. *Biomed Res Int* 2014;**2014**:64164, https://doi.org/10.1155/2014/641647. Epub 2014 Mar 5.

Utratna M, Shaw I, Starr E *et al*. Rapid, transient, and proportional activation of Sigma B in response to osmotic stress in *Listeria monocytogenes*. *Appl Env Microbiol* 2011;**77**:7841–5. https://doi.org/AEM.05732-11

van Schaik W, Zwietering MH, de Vos WM *et al*. Deletion of the *sigB* gene in *Bacillus cereus* ATCC 14579 leads to hydrogen peroxide hyperresistance. *Appl Environ Microb* 2005;**71**:6427–30. https://doi.org/10.1128/aem.71.10.6427-6430.2005

Wemekamp-Kamphuis HH, Wouters JA, de Leeuw PPLA. *et al*. Identification of sigma factor σ^B-controlled genes and their impact on acid stress, High Hydrostatic pressure, and freeze survival in *Listeria monocytogenes* EGD-e. *Appl Environ Microb* 2004;**70**:3457–66. https://doi.org/10.1128/aem.70.6.3457-3466.2004

Wiedmann M, Arvik TJ, Hurley RJ *et al*. General stress transcription factor Sigma B and its role in acid tolerance and virulence of *Listeria monocytogenes*. *J Bacteriol* 1998;**180**:3650–6. https://doi.org/10.1128/JB.180.14.3650-3656.1998

Yadav B, Spinelli AC, Govindan BN *et al*. Cold plasma treatment of ready-to-eat ham: influence of process conditions and storage on inactivation of *Listeria innocua*. *Food Res Int* 2019;**123**:276–85. https://doi.org/10.1016/j.foodres.2019.04.065

Received 21 January 2025; **revised** 23 May 2025; **accepted** 12 July 2025